

# GRAVITY ANOMALIES

**D. C. Mishra**

*National Geophysical Research Institute, Hyderabad, India*

**Keywords:** gravity anomalies, isostasy, Free Air and Bouguer gravity anomalies

## Contents

1. Introduction
2. Free Air and Bouguer Gravity Anomalies
3. Separation of Gravity Anomalies
  - 3.1 Regional and Residual Gravity Fields
  - 3.2 Separation Based on Surrounding Values
  - 3.3 Polynomial Approximation
  - 3.4 Digital Filtering
4. Analytical Operations
  - 4.1 Continuation of the Gravity Field
  - 4.2 Derivatives of the Gravity Field
5. Isostasy
  - 5.1 Isostatic Regional and Residual Fields
  - 5.2 Admittance Analysis and Effective Elastic Thickness
6. Interpretation and Modeling
  - 6.1 Qualitative Interpretation and Some Approximate Estimates
  - 6.2 Quantitative Modeling Due to Some Simple shapes
    - 6.2.1 Sphere
    - 6.2.2 Horizontal Cylinder
    - 6.2.3 Vertical Cylinder
    - 6.2.4 Prism
    - 6.2.5 Contact
  - 6.3 Gravity Anomaly Due to an Arbitrary Shaped Two-dimensional Body
  - 6.4 Basement Relief Model
7. Applications
  - 7.1 Bouguer Anomaly of Godavari Basin, India
  - 7.2 Spectrum and Basement Relief
  - 7.3 Modeling of Bouguer Anomaly of Godavari Basin Along a Profile
  - 7.4 Some Special Applications
- Glossary
- Bibliography
- Biographical Sketch

## Summary

Gravity anomalies are defined in the form of free air and Bouguer anomalies. Various methods to separate them in the regional and the residual fields are described, and their limitations are discussed. Polynomial approximation and digital filtering for this purpose suffer from the arbitrary selection of the order of polynomial and cut off frequency, respectively. However, some constraints on the order of these anomalies can

be imposed to select these parameters judiciously. The regional field is important for delineating deep-seated sources, which are significant for geodynamic studies, while the residual field is important for exploration of minerals, hydrocarbons, engineering geophysics, and other problems related to shallow sources. Analytical operations such as continuation of fields and derivative maps are discussed as means of enhancing the regional and the residual fields and delineating shallow bodies, respectively. Finally, qualitative and quantitative approaches to the interpretation and modeling of gravity data are described, and expressions for the gravity field derived from some simple models and two-dimensional arbitrarily shaped bodies are given. The frequency domain method to compute the basement relief directly from the observed gravity field over sedimentary basins is described. Some of these methods are demonstrated over the Bouguer anomaly of the Godavari Basin, India. At the end, some unconventional applications of gravity anomalies are highlighted, and important references are provided.

## 1. Introduction

The difference between the observed gravity at a place and its theoretical value depending on its latitude is known as a gravity anomaly. It is also referred to spatially as the difference between the gravity fields observed at two points. In geophysics, there are two kinds of gravity anomalies—free air and Bouguer anomalies—depending on type of correction applied to the observed gravity field at the point of observation.

## 2. Free Air and Bouguer Gravity Anomalies

The observed gravity field after correction (corr) for latitude (theoretical gravity) and topography is known as the free air gravity anomaly, or simply the free air anomaly ( $\Delta g_f$ ), which is given by:

$$\Delta g_f = \text{observed gravity} - \text{tidal corr} - \text{theoretical gravity} + \text{topographic corr} + \text{free air corr} \quad (1)$$

If the attraction due to the effect of material between the plane of observation and the m.s.l. (known as the Bouguer correction ( $b_C$ )) is subtracted from the free air anomaly, the corrected gravity field is called the Bouguer gravity anomaly, or simply the Bouguer anomaly or gravity anomaly ( $\Delta g$ ), and given by:

$$\Delta g = \Delta g_f - b_C \quad (2)$$

The Bouguer anomaly is normally for a crustal density of  $2.67\text{g/cm}^3$ . However, one can compute Bouguer anomaly for any other density, such as in the case of sedimentary basins where the Bouguer anomaly for a lower density corresponding to the sediments can be computed. The free air anomaly is found to be more suitable than the Bouguer anomaly in certain cases, such as in oceans, where the free air anomaly is mainly computed, as the plane of observation is same as the m.s.l. It is also found to be useful in assessing isostatic compensation as discussed in the section on isostasy in this article. Free air and Bouguer anomalies computed from the observed gravity field can be plotted as a profile with reference to distance from a fixed reference station, or in a two-

dimensional map if data is recorded in a two-dimensional plane. The contour interval is chosen depending on the accuracy of the gravity data: the contour interval should be approximately 2–3 times the latter. For example, in regional surveys, as the general accuracy of the gravity data is 1–2 mGal, the contour interval is generally 5 mGal. In oil exploration, the contour interval is generally 1 mGal, while in mineral exploration it is 0.1 mGal or 0.01 mGal depending on the nature of surveys. In microgravity surveys, it is generally 0.001 mGal or 1  $\mu$ Gal. A typical gravity profile and map are shown in Figures 1 and 6, respectively.

### 3. Separation of Gravity Anomalies

The gravity field recorded at Earth's surface is the cumulative effect of the sources at different levels. Mostly, the gravity effect of sources from the surface downward, at least up to the Moho, is recorded in these surveys. It is therefore essential to separate the observed field originating from different levels. In general, they are separated broadly in two groups, namely the regional and the residual fields, originating from deep seated and shallow sources, respectively.

#### 3.1 Regional and Residual Gravity Fields

In general, as the name indicates, the regional field is characteristic of the region as a whole and originates from deep-seated sources, while the residual field is confined to a localized area and originates from shallow sources. In prospecting for minerals and oil, the residual field is important, but in crustal studies and geodynamic applications, the regional component of the observed field assumes more significance.

#### 3.2 Separation Based on Surrounding Values

The easiest method to separate the regional and the residual components of the observed gravity field is to smooth the fluctuations based on visual inspection, as shown in Figure 1.

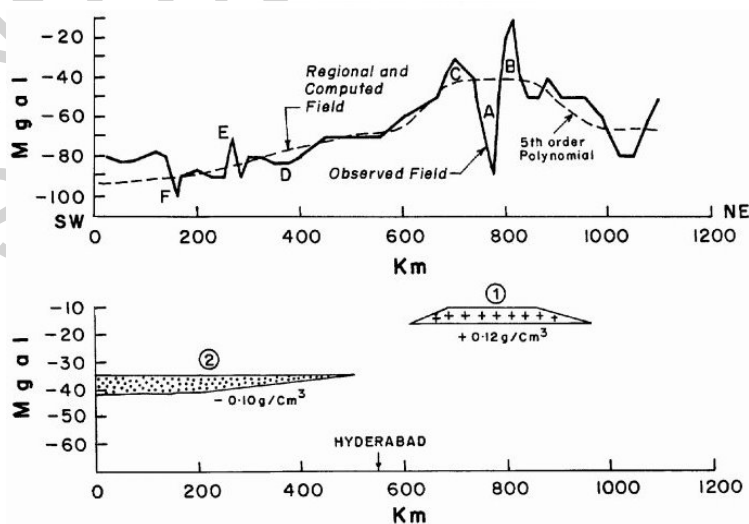


Figure 1. A gravity profile and the regional field based on smoothing of the observed field. The same regional field almost fits with the fifth order polynomial derived from

the observed field. The regional field represents high gravity towards the northeast, decreasing towards the southwest, which is caused by deeper sources (1) and (2). A, B, C, D, E, and F represent the residual field caused mostly by exposed rocks.

This assumes that the values outside the anomalous zone represent a regional field that varies smoothly in the region, while the residual field shows sharp fluctuations. This approach is mostly suitable along profiles.

The other method of regional–residual separation is the graphical method, which is suitable for data recorded over a grid. The observed gravity field surrounding a particular grid point is averaged and subtracted from the central value, which provides the residual field at that point. In this manner, at all grid points a new grid is generated, which is contoured to obtain the residual anomaly map representing shallow sources. This method is dependent on the grid size adopted for averaging the surrounding values, and therefore depends considerably on the individuals experience in dealing with gravity anomalies, and the nature of the problem for which the survey is conducted.

### **3.3 Polynomial Approximation**

In this method, the regional and the residual fields are represented by low and high order surfaces, respectively. The observed gravity anomaly is approximated by a power series. The regional field  $g_r$  along the x-axis can be represented by:

$$g_r = a_0 + a_1 x + a_2 x^2 + a_n x^n \quad (3)$$

where  $n$  is the order of the polynomial being used to approximate the regional field. The coefficients are evaluated using the principles of least squares and the trends of different orders ( $n$ ) are computed. One of the low order trend (say 2, 3, ...) is selected as the regional field, and its difference from the observed field is the residual field. However, the selection of the order of polynomial ( $n$ ) to represent the regional field is quite arbitrary, and depends considerably on the experience of the interpreter. If the depth to the shallow sources (such as basement) is known in certain sections, from seismic profiles or borehole information, some constraints on the order of polynomial can be imposed that will provide the right magnitude of the residual field at these points. For two-dimensional data, surfaces of different order are approximated in the  $(x, y)$  direction over the data grid. Figure 1 shows a fifth order polynomial as the regional field, which almost coincides with the smoothly varying field drawn based on visual inspection as discussed above. In this figure, the regional field shows a gravity “high” towards the northeast and a gravity low towards the southwest, which are caused by deeper sources as indicated by sources (1) and (2) constrained from seismic information from this region. There are several residual anomalies marked as A, B, C, D, E, and F (Figure 1), which are caused by shallow/exposed sources.

### **3.4 Digital Filtering**

Digital filtering of geophysical data is based on the principles of Fourier transform and signal processing. The observed gravity field  $g(x)$  can be represented by discrete Fourier transform in frequency domain as:

$$g(x) = \sum_{f=-n/2}^{n/2} g(f) \exp(2\pi i.f.z/\lambda) \quad (4)$$

where  $f$  is the frequency,  $n$  is the number of observations,  $z$  is the depth to the causative sources,  $\lambda$  is the wavelength, and  $g(f)$  is the transform of the gravity field given by:

$$g(f) = \frac{1}{n} \sum_{x=1}^n g(x) \exp(-2\pi i.f.x/n) \quad (5)$$

$g(f)$  is known as the amplitude spectrum corresponding to frequencies  $f$ , and the corresponding power or energy spectrum is

$$g^2(f) = g(f) g^*(f) \quad (6)$$

where  $*$  denotes complex conjugate.

In practice, equally spaced digital data is generated from the recorded data by interpolation, or alternatively the Bouguer anomaly profile is digitized at equal intervals depending on stations' spacing and depth of investigation. However, the sampling interval should be such that it represents the highest frequency present in the data set, known as the Nyquist frequency, which is equal to  $1/(2 \Delta x)$ , where  $\Delta x$  is the sampling interval. The digital data is transformed into the frequency domain providing the amplitudes of various frequencies (wavelengths) present in the data set. In the case of maps, the two-dimensional version of the discrete Fourier transform is used, and the computed amplitude spectrum can be averaged in concentric circles for similar frequencies to provide the variation of  $g(f)$  with  $f$ , known as the radial spectrum. In these cases,  $f = (k^2 + m^2)^{1/2}$  where  $k$  and  $m$  are frequencies along the  $(x, y)$  axis.

The plot of log of amplitude spectrum versus frequencies (Eqs. 4 and 5) provides straight-line segments corresponding to sources distributed at different levels. A typical plot of amplitude spectrum is shown in Figure 7, which shows three linear segments corresponding to sources distributed at three different levels. The first segment corresponding to low frequencies represents deeper sources compared to other segments corresponding to higher frequencies. In practice, two to three layers can be effectively separated in a spectral plot. Depending on these frequency bands, low and high pass filters can be designed to separate the regional and the residual fields.

The selection of cut-off frequency for low and high pass filters is arbitrary and depends largely on the experience of the interpreter. It is, therefore advisable to design three or four alternatives of these filters, and through trial and error based on other available information and experience, decide the appropriate cut-off frequency/wavelength.

As is apparent from Figure 7, most of the energy is concentrated in the first segment, and therefore it is not possible to assign frequency bands for the regional and the residual fields based on spectral plots as suggested by several workers. It is advisable to assign the first few frequencies (say 1–2 frequencies) to the regional field, and the remaining field represents the residual field.

## 4. Analytical Operations

The observed gravity field can be modified through some mathematical operations, enhancing certain components of the observed field while suppressing the other components. These operations are called analytical operations. The two most important operations are continuation and derivatives of the observed field.

### 4.1 Continuation of the Gravity Field

The field observed in one plane can be continued mathematically upwards or downwards to any other plane. There are several schemes for this purpose; however, the one carried out in the frequency domain discussed below is most simple to apply. As is evident from Eq. (4), the observed field at a level  $z_0$  can be continued to any/other level ( $z_1$ ) by simply multiplying the Fourier coefficients of the observed field by:

$$\sum_{f=-n/2}^{+n/2} \exp[2\pi i f(z_0 - z_1)/\lambda] \quad (7)$$

$z$  being positive in the downward direction. Therefore, the continuation operators for  $\Delta z = z_0 - z_1$  are as follows:

Upward continuation:

$$\sum \exp(2\pi i f/\lambda) (-\Delta z) \quad (8)$$

Downward continuation:

$$\sum \exp(2\pi i f/\lambda) (\Delta z) \quad (9)$$

Eqs. (8) and (9) are known as continuation operators. They show that the downward continuation operator increases exponentially with depth and is therefore unstable for large  $\Delta z$ , while continuation upward is a stable operation.

Further, the amplitudes of the high frequency (short wavelength) component (Figure 2b) increases much more than the low frequency component (Figure 2a) while continuing downwards. Therefore, the high frequency component, which usually represents noise, gets much more enhanced while continuing the fields downwards.

This produces oscillations in the downward continued field, and imposes a certain limit beyond which the fields cannot be continued downwards. It is, therefore, advisable to filter high frequency components, which represent noise, before continuing the field downwards.

Conversely, continuation upward enhances low frequency components originating from deeper levels than high frequency components (Figure 2a). Therefore, the continuation upwards and downwards can be seen as means of enhancing the regional and the residual fields respectively.

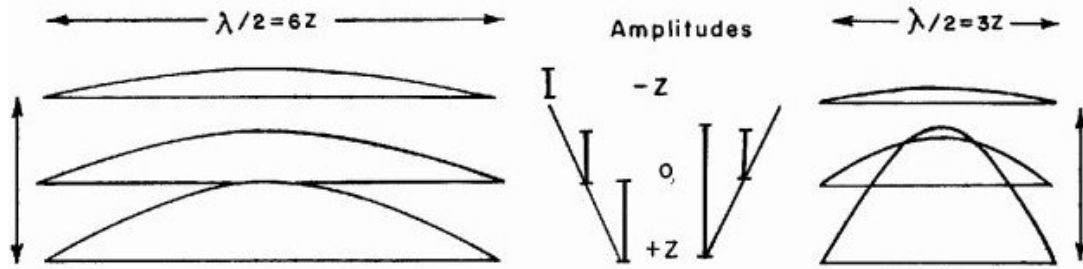


Figure 2. Continuation upwards and downwards by one unit of depth,  $z$ , for a wavelengths of (a)  $12z$  and (b)  $6z$

#### 4.2 Derivatives of the Gravity Field

Derivatives of the gravity field have been popular with geophysicists as they suppress low frequency components and enhance high frequency components, thus delineating shallow bodies. As in the case of continuation of fields, different work to compute the first and second derivatives of the gravity field has provided several sets of coefficients. However, the operations in the frequency domain for this purpose, as in the case of the continuation operator, are simple and easy to perform. Differentiating equation (4) gives:

$$\frac{\partial g(x)}{\partial z} = \sum_{f=-n/2}^{n/2} g(f)(f) \exp(-2\pi ifz) / \lambda \quad (10)$$

In Eq. (10),  $f$  can be regarded as a filter function for the first derivative. Similarly, for the second derivative and for the  $n$ th derivative, the filter functions are  $(f^2)$  and  $(f^n)$ , respectively. Therefore, any derivative of the observed field can be computed through the simple filter operations given above. The second derivative map tends to define the outline of bodies through its zero contour. Therefore, is widely used in prospecting to define different shallow bodies in a region.

-  
-  
-

TO ACCESS ALL THE 26 PAGES OF THIS CHAPTER,  
Visit: <http://www.eolss.net/Eolss-sampleAllChapter.aspx>

#### Bibliography

- Gibson R. I. and Milligan P. S. (1998). *Geological application of gravity and magnetics, Case Histories*. USA: SEG Publication. [Several applications of these methods are illustrated.]
- Hahn A. (1965). Two applications of Fourier analysis for the interpretation of geomagnetic anomalies. *Journal of Geomagnetism and Geoelectricity* **17**, 195–225. [Provides theory for Fourier transformation of

potential fields.]

Hahn A., Kind E. G., and Mishra D. C. (1976). Depth estimation of magnetic sources by means of Fourier amplitude spectra. *Geophysical Prospecting* **24**, 287–308. [Provides theory for depth estimation from Fourier amplitude spectra and separation of observed potential field into field originating from different depths.]

Hare J. L., Ferguson J. F., and Aiken C. L. V. (1999). The 4-D microgravity method for waterflood surveillance. A model study for the Prudhoe Bay reservoir, Alaska. *Geophysics* **64**, 78–97. [An unconventional application of gravity method.]

Li X., and Chouteau M. (1998). Three-dimensional gravity modeling in all space. *Surveys in Geophysics* **19**, 339–368. [Provides a review of various approaches for computing the gravity field due to three-dimensional bodies.]

Mckenzie D. and Fairhead D. (1997). Estimate of the effective elastic thickness of the continental lithosphere from Bouguer and free air gravity anomalies. *Journal of Geophysical Research* **102**(27), 523–552. [Provides theory for admittance analysis.]

Mishra D. C., Singh B., Tiwari V. M., Gupta S. B., and Rao M. B. S. V. (2000). Two cases of continental collisions and related tectonics during the Proterozoic period in India: Insights from gravity modeling constrained by seismic and magnetotelluric studies. *Precambrian Research* **99**, 149–169. [Application of gravity method to collision tectonics in Proterozoic terrain.]

Mishra D. C., Chandrasekhar D. V., Venkat Raju D. Ch., and Vijaya Kumar V. (1999). Crustal structure based on gravity magnetic modeling constrained from seismic studies under Lambert rift, Antarctica and Godavari and Mahanadi rifts, India and their interrelationship. *Earth and Planetary Science Letters* **172**, 287–300. [Crustal structures based on modeling of gravity profiles across rift basins and their application to geodynamics.]

Parasnis D. S. (1997). *Principles of Applied Geophysics*. 429 pp. London: Chapman and Hall. [This book deals with the various geophysical methods including gravity methods.]

Pedersen L. B. (1979). Constrained inversion of potential field data. *Geophysical Prospecting* **27**, 726–748. [Inversion theory applied to model gravity anomalies.]

Radhakrishnamurthy I. V. (1998). Gravity and magnetic interpretation in exploration geophysics. *Memoir Geological Society of India* **40**. Bangalore, India. [Provides computer packages on a floppy to compute the gravity field due to different bodies including two- and three-dimensional arbitrarily shaped bodies.]

Tiwari V. M. and Mishra D. C. (1997). Microgravity changes associated with continuing seismic activities in Koyna area, India. *Current Science* **73**, 376–381. [Application of microgravity measurements in a seismically active region is demonstrated.]

Tiwari V. M. and Mishra D. C. (1999). Estimation of effective elastic thickness from gravity and topography data under the Deccan volcanic province, India. *Earth and Planetary Science Letters* **171**, 289–299. [Demonstrates the application of effective elastic thickness with reference to the seismogenic layer in the crust.]

Webring M. (1986). Saki, a Fortran program for generalized linear inversion of gravity magnetic profile. *Open file report, US* **45**, 85–112. [This computer package is available from the United States Geological Survey, USA for computation of gravity and magnetic anomalies due to two and a half dimensional bodies.]

## Biographical Sketch

**Dr. D. C. Mishra**, was born in 1943 and completed M.Sc. (geophysics) in 1963 at Banaras Hindu University (BHU), India. He worked on rock magnetism in Tata Institute of Fundamental Research, Bombay, and was awarded a Ph.D. in 1966 from B.H.U. where he was a lecturer in the Department of Geophysics. He joined National Geophysical Research Institute, Hyderabad in 1966, first as post doctoral fellow and then as a scientist, and since then has been working in this institute in various capacities. For the last 20 years he has been head of the various projects on gravity and magnetic surveys in India. He was also associated with airborne magnetic surveys and modeling of satellite magnetic and gravity data

over India and adjoining oceans. In between, he was associated for a few years with the Federal Institute of Geosciences, Hannover, Germany and the Department of Geophysics, University of Arhus, Denmark as a post doctoral fellow. He is a fellow of the Indian Geophysical Union and Association of Exploration Geophysics, India.

UNESCO – EOLSS  
SAMPLE CHAPTERS